



This is a repository copy of *A novel dual-sided PM variable flux memory machine*.

White Rose Research Online URL for this paper:
<http://eprints.whiterose.ac.uk/139340/>

Version: Accepted Version

Article:

Yang, H., Lin, H., Zhu, Z.Q. orcid.org/0000-0001-7175-3307 et al. (2 more authors) (2018)
A novel dual-sided PM variable flux memory machine. IEEE Transactions on Magnetics, 54 (11). 8110605. ISSN 0018-9464

<https://doi.org/10.1109/TMAG.2018.2845870>

© 2018 IEEE. Personal use of this material is permitted. Permission from IEEE must be obtained for all other users, including reprinting/ republishing this material for advertising or promotional purposes, creating new collective works for resale or redistribution to servers or lists, or reuse of any copyrighted components of this work in other works. Reproduced in accordance with the publisher's self-archiving policy.

Reuse

Items deposited in White Rose Research Online are protected by copyright, with all rights reserved unless indicated otherwise. They may be downloaded and/or printed for private study, or other acts as permitted by national copyright laws. The publisher or other rights holders may allow further reproduction and re-use of the full text version. This is indicated by the licence information on the White Rose Research Online record for the item.

Takedown

If you consider content in White Rose Research Online to be in breach of UK law, please notify us by emailing eprints@whiterose.ac.uk including the URL of the record and the reason for the withdrawal request.



eprints@whiterose.ac.uk
<https://eprints.whiterose.ac.uk/>

A Novel Dual-Sided PM Variable Flux Memory Machine

Hui Yang¹, *Member, IEEE*, Heyun Lin¹, *Senior Member, IEEE*, Z. Q. Zhu², *Fellow, IEEE*, Shukang Lyu¹, and Keyi Wang¹

¹School of Electrical Engineering, Southeast University, Nanjing 210096, P. R. China

²Department of Electronic and Electrical Engineering, University of Sheffield, Sheffield S1 3JD, U.K.

This paper proposes a novel dual-sided permanent magnet memory machine (DSPM-MM) by combing the distinct advantages of “high torque density” of conventional rotor-PM machine and “convenient online PM flux control” of stator-PM MM. In the proposed design, the consequent-pole NdFeB PMs are placed in the rotor, while low coercive force (LCF) PMs are mounted between the adjacent stator teeth to enable flexible air-gap flux adjustment. Meanwhile, since the LCF PMs can be either remagnetized or demagnetized bi-directionally by a current pulse, the associated flux-weakening (FW) copper loss is eliminated, and hence the proposed DSPM-MM can maintain high efficiency operation over a wide operating range. The machine topology and operating principle are introduced and addressed from perspective of the nonlinear hysteresis behavior of LCF PMs, as well as dual flux modulation effect, respectively. Then, the electromagnetic characteristics of the proposed machines having various available rotor poles are investigated and compared. The feasibility of the proposed design is validated by both finite-element (FE) and experimental results.

Index Terms—Consequent pole, dual-sided, hybrid permanent magnet (PM), memory machine, variable flux.

I. INTRODUCTION

DUE TO the merits of high torque density and high efficiency, permanent magnet (PM) machines are extensively recognized as a promising candidate for electric vehicle (EV) applications [1]. Nevertheless, the non-adjustable air-gap flux is a major concern for the conventional rare-earth PM machines. This will lead to a limited constant-power speed range (CPSR). Meanwhile, the required d -axis flux-weakening (FW) current and the associated high copper loss at high speed inevitably degrade the efficiency over the whole driving cycle, which is adverse to traction applications. In general, the conventional PM machines suffer from the conflicted low-speed high torque and high-speed high power capabilities. From this viewpoint, it is advisable to control the magneto motive forces (MMF) of PMs to meet the specific requirement at different loads and speeds [2].

Recently, the concept of “memory machine (MM)” has been proposed and recognized as a “true” flux adjustable machine particularly suitable for wide speed operation [3]. The flexible air-gap flux adjustment can be achieved by applying a current pulse to either remagnetize or demagnetize low coercive force (LCF) PMs. Consequently, their magnetization state (MS) can be “memorized” by a certain current pulse level, allowing FW control current to be greatly reduced and the corresponding losses minimized. Thus, high efficiency can be maintained within a wide operating speed/load range. In addition, since back electromotive force (EMF) of MM can be controlled due to the variable flux property so that the CPSR can be further extended within the inverter voltage constraint by purposely demagnetizing the LCF PMs at high speed cases [4].

Generally, the existing VFMMs can be divided into AC- and DC-magnetized types according to the current pulse pattern. The former employs the stator armature winding to energize d -axis current pulse to achieve online MS control [3]-[6]. Nevertheless, for those structures, LCF magnets mounted on the rotor are generally susceptible to armature reaction fields. In addition, the high requirements for the current decoupling control and the rotor positing make the online magnetization

relatively sophisticated. On the other hand, the MM concept was extended to stator-PM structures, forming several newly emerged topologies [7]-[13] having both PMs and DC coils on the stationary side. In these cases, the current pulses are produced by the DC magnetizing coils, which facilitate the online MS manipulation. In addition, the thermal dissipation can be conveniently managed, and unintentional demagnetization posed by the armature reaction can be well prevented. Nevertheless, the fact that two kinds of PMs, i.e., NdFeB and LCF PMs, as well as two sets of windings are located on stator leading to excessively crowded stator space and low torque density. Overall, since the existing MMs simply employ low-magnetic-product LCF PMs to partially or totally replace NdFeB PMs regardless of AC- and DC-magnetized topologies, their torque densities are still lower than the conventional PM machines. This is widely regarded as a very challenging issue for designing MMs applicable for traction applications [11].

To resolve the abovementioned drawback, a novel dual-sided permanent magnet memory machine (DSPM-MM) is proposed in this paper, which can be geometrically considered as a combination of conventional rotor rare-earth machine and DC-magnetized MM having LCF PMs on the stator. Thus, the proposed DSPM-MM can combine the distinct synergies of high torque density and convenient online magnetization state (MS) manipulation. Meanwhile, high efficiency operation can be well maintained over a wide operating speed/load range. The machine configuration and operating principle are described and addressed, respectively. In addition, the electromagnetic characteristics of the proposed machine having various available rotor poles are analyzed and compared by finite-element (FE) method. The experimental tests are carried out on a 6-stator-PM/7-rotor-PM prototype, which verifies the feasibility of the proposed design.

II. MACHINE CONFIGURATION AND OPERATING PRINCIPLE

A. Machine Configuration

Fig. 1 shows the topology of the proposed DSPM-MM with 6-stator-PM/7-rotor-PM arrangement, which is characterized

by a combination of two single-sided machines having two kinds of magnets on rotating and stationary sides, respectively. For the rotor, the homopolar NdFeB PMs and iron poles are the alternately arranged, forming a consequent-pole configuration. For the stator, the LCF PMs are alternately buried in air space between adjacent stator tooth poles, and the LCF magnets are encircled by the DC magnetizing coils.

The developed machine combines the distinct advantages of the conventional rare-earth machine and stator-PM MM, which can be summarized as follows:

1) The merits of high torque density in conventional rotor-PM machine and easy magnetization control in stator-PM MM can be well synthesized;

2) The wide speed range and high efficiency at CPSR can be realized due to excellent flux adjusting capability and negligible FW copper loss.

3) The ferromagnetic stator and rotor iron poles provide an effective circulating path for the armature fields as well as the magnetizing fields generated by the current pulse. That is to say, the parallel PMs and armature reaction fields can prevent the LCF PMs from unintentional armature demagnetization.

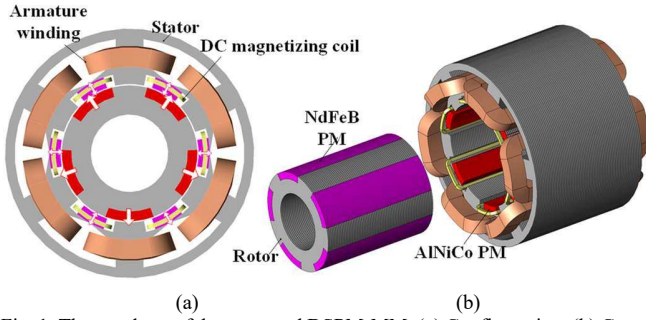


Fig. 1. The topology of the proposed DSPM-MM. (a) Configuration. (b) Cross-sectional view.

B. Operating Principle

1) Variable Flux Principle

Firstly, the variable flux principle of the proposed DSPM-MM can be characterized by a simplified illustration of the hysteresis model of LCF PMs as shown in Fig. 2 [13]. It can be seen that the coercive force of LCF PM is much lower than that of NdFeB. Thus, the PM working point can be repetitively shifted between different recoil lines by temporarily applying remagnetizing or demagnetizing current pulse. For instance, the working point of the PM is initiated at P_1 , which is the cross point of the load line and the demagnetizing curve. When applying a demagnetizing current pulse, the working point will descend to G . After the withdrawal of the current pulse, the working point will move along a new recoil line and stabilize at new working point P_2 . On the other hand, when a remagnetizing current pulse is applied, the working point of the PM will track the trajectory of $CDEB$ and return to P_1 .

Furthermore, the proposed DSPM-MM can combine high torque density of conventional constant PM flux machine with variable PM flux characteristics for manipulating losses and high efficiency distributions within a duty-cycled operation. As a result, the NdFeB PMs serve as a dominant contributor for air-gap flux, while the LCF PMs work as a flux adjustor. The

effective flux linked with the armature windings can be strengthened or weakened when the magnetization directions of LCF magnets are identical or opposite to those of NdFeB PMs, i.e., so-called the flux-enhanced and flux-weakened states, as illustrated in Fig. 3. Therefore, for low-speed region, NdFeB and LCF PMs are with identical magnetization direction, the torque density can be subsequently improved. On the other hand, for high-speed region, the LCF PMs are reversely demagnetized to short-circuit and weaken the NdFeB PM fields, and hence the CPSR can be effectively extended within the limitation of the inverter power rating.

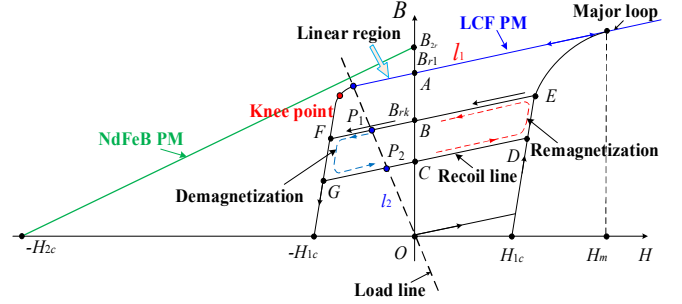


Fig. 2. Flux-adjusting principle illustrated by the simplified hysteresis model.

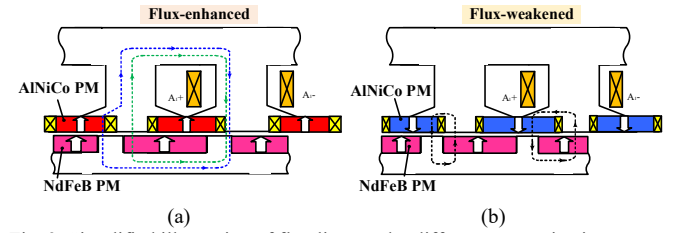


Fig. 3. Simplified illustration of flux lines under different magnetization states. (a) Flux-enhanced state. (b) Flux-weakened state.

2) Bidirectional Flux Modulation Effect

Since the proposed DSPM-MM can be considered as the combination of two separate machines having PMs on either stationary or rotary parts, its operating principle can be understood from the perspective of the resultant dual flux modulation effects arising from dual-sided PM excitations [15]-[16].

For the rotor side, the dominant air-gap flux density due to the PM MMF modulated by the stator teeth can be approximately expressed as

$$B_{\delta} = F_m \Lambda_{total} \approx \frac{4B_r h_{rm}}{\mu_0 \mu_r} \Lambda_0 \cos[p_m(\theta - \omega_{rm}t - \theta_0)] + \frac{2B_r h_{rm}}{\mu_0 \mu_r} \Lambda_1 \cos\left((p_m - p_{sm})\left(\theta - \frac{p_m(\omega_{rm}t - \theta_0)}{p_m - p_{sm}}\right)\right) \quad (1)$$

where F_m , B_r , μ_0 , μ_r , h_{rm} , and Λ_{total} are the PM MMF, recoil flux density, vacuum permeability, PM relative permeability, rotor PM thickness and total air-gap permeance, respectively; ω_{rm} , θ , and θ_0 are the rotating angular speed of rotor, the circumferential position and initial position, respectively. The first term in (1) is the fundamental component similar to the conventional rare-earth machines, while the second term can be considered as the modulated one. The steady torque can be produced due to the synchronization of the modulated low-order harmonic with high velocity and its corresponding coil

MMF one, as long as the pole pair number and angular speed of working spatial harmonic p_{w1} and ω_{w1} satisfy

$$p_{w1} = |p_{sm} - p_{rm}| \quad (2)$$

$$\omega_{w1} = -\frac{p_{rm}}{p_{sm} - p_{rm}} \omega_r = -G_r \omega_{rm} \quad (3)$$

where the “minus” sign indicates that this modulated harmonic rotates reversely with the fundamental one. Thus, the second term in (1) can effectively contribute to torque transmission.

The flux modulation effect of the stationary PM fields can be analyzed in a similar manner as the rotor side. The stationary PM fields (PPN= p_{sm}) are modulated by the rotating poles with (PPN= p_{rm}), and hence the angular speed of working harmonic ω_{w2} can be represented by

$$\omega_{w2} = \frac{p_{rm}}{p_{rm} - p_{sm}} \omega_r = -G_r \omega_{rm} \quad (4)$$

It can be derived from (3) and (4) that the working harmonics of the individual case share the same PPN and rotating speed. Thus, the stable torque transmission can be achieved. As a result, the effective couplings between the armature reaction fields and magnetic fields excited by either rotor or stator PMs can be synthesized, i.e., the dual flux modulation effects [15]-[16]. This effect can be further reflected by the similar flux line patterns excited by only stator PM, rotor PM and dual-sided PM (see Fig. 4), as well as the open-circuit phase flux linkages produced by the stator PMs, the rotor PMs, dual-sided PMs, and the synthetic result by stator/rotor-PMs. (see Fig. 5)

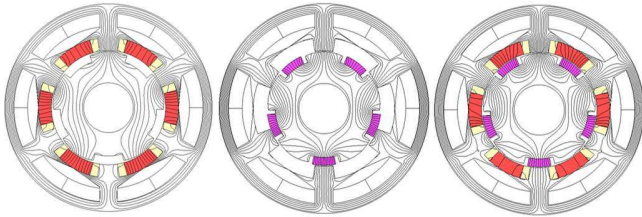


Fig. 4. The open-circuit flux lines excited by (a) the stator PMs, (b) the rotor PMs, and (c) dual-sided PMs.

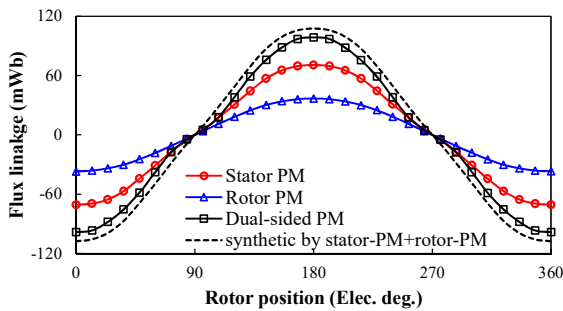


Fig. 5. Phase flux linkage waveforms produced by the stator PMs, the rotor PMs, dual-sided PMs, and the synthetic result by stator/rotor-PMs.

III. ELECTROMAGNETIC CHARACTERISTICS COMPARISON OF DSPM-MMS WITH VARIOUS ROTOR POLES

The feasible rotor pole numbers of the 6-stator-slot DSPM-MMs can be selected as N_r is more close to the multiple of N_s , since the maximum winding factor can be obtained in those cases [17]. Thus, based on 2-D FE analysis, the electromagnetic characteristics of the proposed DSPM-MMs with 4, 5, 7, and 8 rotor poles are evaluated and compared. The design parameters

of the machines are optimized in order to obtain the torque with the copper loss constraint of 30W and zero d -axis current control under the flux-enhanced state.

TABLE I

MAJOR DESIGN PARAMETERS OF PROPOSED 6 STATOR POLE DSPM-MM				
Rotor pole number	4	5	7	8
Rated speed (r/min)	400			
Phase number	3			
Rated current (Arms)	10			
Stator outer diameter (mm)	100			
Air-gap length (mm)	0.5			
Inner diameter of stator (mm)	52.0	54.0	55.0	57.0
Stator tooth width (mm)	7	8	8.5	8.6
LCF PM thickness (mm)	5.5			
LCF PM width (deg.)	24			
Stator back iron height (mm)	3	3.2	3.2	3.5
Rotor pole arc (deg.)	24	22	14	11
LCF magnet grade	AlNiCo-9			
NdFeB magnet grade	N35SH			
Active stack length (mm)	50			
Turns of winding per phase	132			
Turns of per magnetizing coil	100			

A. Flux Regulation Capability

Fig. 6 shows the open-circuit field distributions of the proposed machine under different MSs of LCF PMs. The corresponding phase back-EMF magnitudes (400 r/min) under different MSs is shown in Fig. 7. It can be observed that the field distributions vary more significantly with increasing rotor pole number. That is to say, the 8-rotor-PM machine exhibits the widest MS control range, as reflected in Fig. 10. This is mainly attributed to the fact that more rotor iron poles are beneficial for the magnetic short-circuiting between dual-sided PM fields at the flux-weakened state.

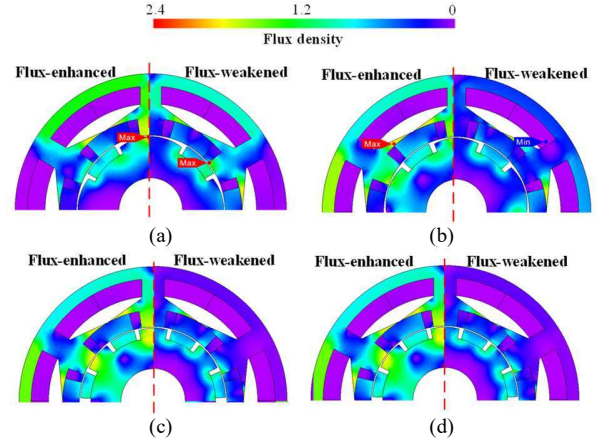


Fig. 6. Open-circuit field distributions under different magnetization states. (a) 4-rotor-PM. (b) 5-rotor-PM. (c) 7-rotor-PM. (d) 8-rotor-PM.

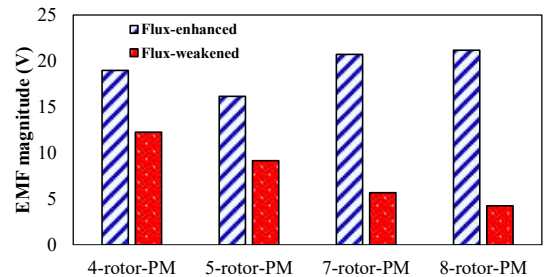


Fig. 7. Comparison of FE predicted back-EMF fundamental magnitudes under different magnetization states, 400r/min.

B. Torque Performance

The steady torque waveforms of the DSPM-MMs with different rotor poles are compared in Fig. 8. It shows that the even-rotor-PM machines exhibit much higher average torques and torque ripples than the odd-rotor-PM counterparts. The large torque ripple issue is mainly resulted by higher EMF harmonics existing in ever-rotor-PM structures [16]. Moreover, the 8-pole-PM machine exhibits the highest torque capability under rated load operation, followed by the 4-rotor-PM one, while the lowest torque capability can be observed in the 5-rotor-PM counterpart.

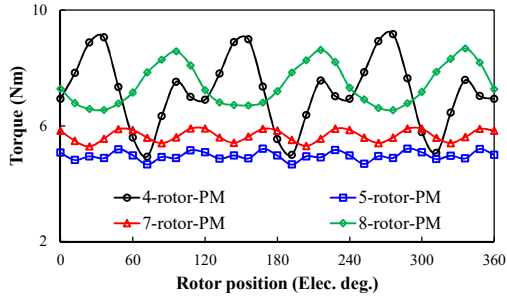


Fig. 8. Comparison of FE predicted steady-torque waveforms under different magnetization states, phase current=10Arms.

C. Efficiency Maps

Due to the satisfactory torque quality and wide MS control range, the 6-stator-PM/7-rotor-PM DSPM-MM is selected for the following investigation. The efficiency maps with different MSs are plotted in Fig. 9. The results confirm that the proposed machine can achieve high efficiency within a wide range of speeds and loads by choosing appropriate MS under different operating regions.

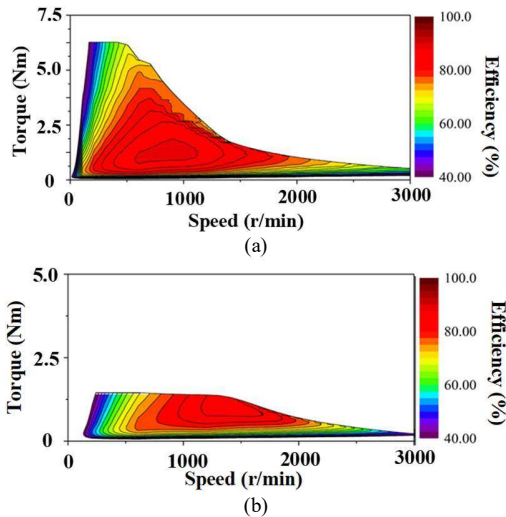


Fig. 9. Efficiency maps . (a) Flux-enhanced. (b) Flux-weakened. (DC link voltage=40 V, rated RMS current=10A)

IV. EXPERIMENTAL VALIDATION

The 6-stator-PM/7-rotor-PM DSPM-MM prototype is manufactured and tested to experimentally validate the foregoing FE results. The prototype and test bench are shown in Fig. 10, where the ONOSOKKI TS-7700 Torque Station is utilized to generate a load torque. The FE-predicted and measured open-circuit back-EMF waveforms at 400r/min under

the different MSs are shown in Fig. 11. It can be observed that the measured results agree well with the FE results, and the satisfactory flux adjusting capability can be obtained, which is advantageous to wide-speed-range applications. In addition, Fig. 12 shows the predicted and measured torque versus current characteristics. It demonstrates that the FE predictions are slightly higher than measurement due to the fact the end effect and manufacturing tolerance are neglected in the FE analysis.

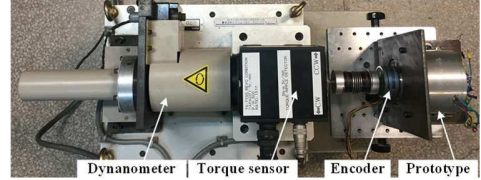


Fig. 10. DSPM-MM prototype and test bench.

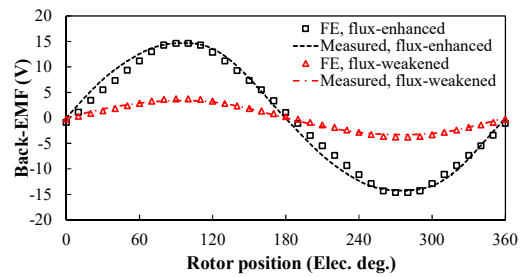


Fig. 11. Comparison of predicted and measured back-EMF waveforms under different magnetization states, 400r/min.

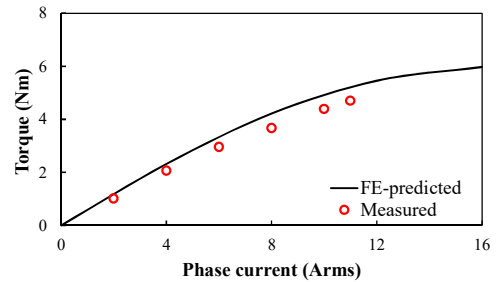


Fig. 12. Comparison of predicted and measured torque against current characteristics under the flux-enhanced states.

V. CONCLUSIONS

This paper proposes a novel DSPM-MM having LCF PMs and NdFeB on the stator and rotor sides, respectively. The machine topology and operating principle are introduced from a perspective of its decomposition into a rotor rare-earth machine and a stator-PM MM respectively. It shows the proposed machine can provide the flexible air-gap flux regulation due to the nonlinear hysteresis characteristics of LCF PMs, as well as the dual flux modulation effect to improve the torque density. In addition, the electromagnetic performance comparison of the proposed machines having various available rotor poles is presented. It can be found that the flux adjusting range is improved with increasing the rotor poles, while the even-rotor-PM machines exhibit higher average torques as well as larger torque ripples than the odd-rotor-PM counterparts. Overall, the 6/7-pole DSPM-MM shows satisfactory torque quality and wide flux adjusting capability, which is chosen for prototype manufacturing. The theoretical analyses and FE results are both verified by the experimental tests.

ACKNOWLEDGMENT

This work was jointly supported in part by National Natural Science Foundations of China under Grant 51377036 and 51377020, in part by Natural Science Foundation of Jiangsu Province for Youth (BK20170674), in part by Specialized Research Fund for the Doctoral Program of Higher Education of China (20130092130005), and in part by the Fundamental Research Funds for the Central Universities (2242017K41003).

REFERENCES

- [1] K. T. Chau, C. C. Chan, and C. Liu, "Overview of permanent-magnet brushless drives for electric and hybrid electric vehicles," *IEEE Trans. Ind. Electron.*, vol. 55, no. 6, pp. 2246-2257, Jun. 2008.
- [2] H. Yang, Z. Q. Zhu, H. Lin, and W. Q. Chu, "Flux adjustable permanent magnet machines: a technology status review," *Proc. CJEE*, vol. 2, no.2, pp.14-30, Dec. 2016.
- [3] V. Ostovic, "Memory motors," *IEEE Ind. Appl. Mag.*, vol. 9, no. 1, pp. 52-61, Jan./Feb. 2003.
- [4] A. Athavale, K. Sasaki, B. S. Gagas, T. Kato, and R. Lorenz, "Variable flux permanent magnet synchronous machine (VF-PMSM) design methodologies to meet electric vehicle traction requirements with reduced losses," *IEEE Trans. Ind. Appl.*, vol. 53, no. 5, pp. 4318-4326, Sep./Oct. 2017.
- [5] H. Hua, Z. Q. Zhu, A. Pride, R. P. Deodhar, and T. Sasaki, "A novel variable flux memory machine with series hybrid magnets," *IEEE Trans. Ind. Appl.*, vol. 53, no. 5, pp. 4396-4405, Sept./Oct. 2017.
- [6] M. Ibrahim, L. Masisi, and P. Pillay, "Design of variable flux permanent magnet machine for reduced inverter rating," *IEEE Trans. Ind. Appl.*, vol. 51, no. 5, pp. 3666-3674, Sep./Oct. 2015.
- [7] B. Kim and T. A. Lipo, "Operation and design principles of a PM vernier motor," *IEEE Trans. Ind. Appl.*, vol. 50, no. 6, pp. 3656-3663, Nov./Dec. 2014.
- [8] Z. Z. Wu, and Z. Q. Zhu, "Analysis of air-gap field modulation and magnetic gearing effects in switched flux permanent magnet machines," *IEEE Trans. Magn.*, vol. 51, no. 5, Article. 8105012, May. 2015.
- [9] C. Yu and K. T. Chau, "Design, analysis, and control of DC-excited memory motors," *IEEE Trans. Energy Convers.*, vol. 26, no. 2, pp. 479-489, Jun. 2011.
- [10] Y. Gong, K. T. Chau, J. Z. Jiang, C. Yu, and W. Li, "Analysis of doubly salient memory motors using preisach theory," *IEEE Trans. Magn.*, vol. 45, no. 10, pp. 4676-4679, Oct. 2009.
- [11] X. Zhu, Z. Xiang, L. Quan, W. Wu, and Y. Du, "Multimode optimization design methodology for a flux-controllable stator permanent magnet memory motor considering driving cycles," *IEEE Trans. Ind. Electron.*, vol. 65, no. 7, pp. 5353-5366, Jul. 2018.
- [12] H. Yang, H. Y. Lin, Z. Q. Zhu, D. Wang, S. Fang, and Y. Huang, "A variable-mode stator consequent pole memory machine," *AIP Advances*, vol. 8, no. 5, Article no: 056612, May. 2018.
- [13] H. Yang, H. Lin, J. Dong, J. Yan, Y. Huang, and S. Fang, "Analysis of a novel switched-flux memory motor employing a time-divisional magnetization strategy," *IEEE Trans. Magn.*, vol. 50, no. 2, pp. 849-852, Feb. 2014.
- [14] L. Jian, Y. Shi, C. Liu, G. Xu, Y. Gong, and C. C. Chan, "A novel dual-permanent-magnet-excited machine for low-speed large-torque applications," *IEEE Trans. Magn.*, vol. 49, no. 5, pp. 2381-2384, May. 2013.
- [15] S. Niu, S. L. Ho, and W. N. Fu, "A novel stator and rotor dual PM vernier motor with space vector pulse width modulation," *IEEE Trans. Magn.*, vol. 50, no. 2, pp. 805-808, Feb. 2014.
- [16] J. T. Chen, and Z. Q. Zhu, "Winding configurations and optimal stator and rotor pole combination of flux-switching PM brushless AC machines," *IEEE Trans. Energy Convers.*, vol. 25, no. 2, pp. 0885-8969, Jun. 2010.

